Revision 1

Volatile abundances of coexisting merrillite and apatite in the martian meteorite Shergotty: Implications for merrillite in hydrous magmas

Francis M. McCubbin[1], Charles K. Shearer[1], Paul V. Burger[1], Erik H. Hauri[2], Jianhua Wang[2], Stephen M. Elardo[1], and James J. Papike[1]

[1]Institute of Meteoritics, Department of Earth & Planetary Sciences, University of New Mexico, Albuquerque, NM 87131, USA

[2]Department of Terrestrial Magnetism, Carnegie Institution of Washington, 5241 Broad Branch Rd., N.W, Washington, DC 20015, USA

Abstract

Whitlockite and merrillite are two Ca-phosphate minerals found in terrestrial and planetary igneous rocks, sometimes coexisting with apatite. Whitlockite has essential structural hydrogen, and merrillite is devoid of hydrogen. Whitlockite components have yet to be discovered in samples of extraterrestrial merrillite, despite evidence for whitlockite-merrillite solid solution in terrestrial systems. The observation of merrillite in meteoritic and lunar samples has led many to conclude that the magmas from which the merrillite formed were "very dry". However, the Shergotty martian meteorite has been reported to contain both apatite and merrillite, and recently the apatite has been shown to contain substantial OH abundances, up to the equivalent of 8600 ppm H_2O. In the present study, we determined the abundances of F, Cl, H_2O, and S in merrillite from Shergotty using secondary ion mass spectrometry (SIMS). We determined that the merrillite in Shergotty was properly identified (i.e., no discernible whitlockite component), and it coexists with OH-rich apatite. The absence of a whitlockite component in Shergotty merrillite and other planetary merrillites may be a consequence of the limited thermal stability of H in whitlockite (stable only at T <1050 °C), which would prohibit merrillite-whitlockite solid-solution at high temperatures. Consequently, the presence of merrillite should not be used as evidence of dry magmatism without a corresponding estimate of the T of crystallization. In fact, if a whitlockite component in extra-terrestrial merrillite is discovered, it may indicate formation by or equilibration with hydrothermal or aqueous fluids.

Keywords: Water on Mars, martian meteorite, SIMS, whitlockite, phosphates

Introduction

Apatite $Ca_5(PO_4)_3(F,Cl,OH)$, merrillite $Ca_{18}Na_2Mg_2(PO_4)_{14}$, and whitlockite $Ca_9(Mg,Fe^{2+})(PO_4)_6[PO_3(OH)]$ are the primary phosphate minerals found in most planetary materials including rocks from Earth, Moon, Mars, and asteroids (Rubin, 1997; Piccoli and Candela, 2002; Jolliff et al., 2006; Hughes et al., 2008). For many years, the terms merrillite and

whitlockite have been used interchangeably in the meteorite literature. Much of the confusion regarding the relationship between terrestrial and extraterrestrial "whitlockite" is based on the presence or absence of hydrogen in the mineral structure. Whitlockite has approximately 8500 ppm H_2O, and the term "merrillite" has been adopted to identify the hydrogen-free form of whitlockite (Jolliff et al., 2006). The atomic structures of merrillite and whitlockite were examined in detail by Hughes et al. (2006, 2008). On Earth, whitlockite has been found in rocks from evolved pegmatitic systems (Frondel, 1941; Calvo and Gopal, 1975; Jolliff et al., 2006; Hughes et al., 2008) and in some mantle rocks (i.e., Ionov et al., 2006). Furthermore, terrestrial whitlockite has been shown to have some merrillite component (Hughes et al., 2008). For the meteoritic and lunar materials that have been investigated, merrillite appears to be far more common than whitlockite, and it has been proposed that the whitlockite component is unique to terrestrial samples (Hughes et al., 2008). There are some reports of "whitlockite" in the meteorite literature; however, these likely represent misidentifications of merrillite because there have been no reports of extraterrestrial whitlockite that have been verified through structural studies or analyzed for their H_2O or F contents (F-endmember form of whitlockite is bobdownsite with 1.8 wt.% F; Tait et al., 2011). Hughes et al. (2006) reported the atomic arrangement of lunar merrillite (from Jolliff et al., 1993) and demonstrated that the phase is similar to meteoritic merrillite and, predictably, devoid of hydrogen. In a follow-up study, Hughes et al. (2008) reported the atomic arrangements of two natural samples of whitlockite, one synthetic whitlockite, and samples of synthetic whitlockite that were heated at 500 °C and 1050 °C for 24 hours. The crystal chemistry and crystal structures of the phases were compared, and it was discovered that the latter treatment resulted in the dehydrogenation of whitlockite to form merrillite. It was pointed out in that study that the existence of merrillite in meteoritic and lunar

rocks is not surprising because these materials are known to crystallize in environments in which hydrogen is rare or absent. In fact, the presence of merrillite vs. whitlockite is widely thought to serve as an indication that magmas are anhydrous (i.e., Smith and Hervig, 1979; Sha, 2000; Ionov et al., 2006; Patiño Douce and Roden, 2006; Hughes et al., 2008; Patiño Douce et al., 2011).

Recent evidence has challenged the notion that planetary magmas are anhydrous. Substantial evidence has been presented to show that lunar magmas have higher H contents than previously suggested (Saal et al., 2008, 2013; McCubbin et al., 2010b, 2010c; Boyce et al., 2010; Greenwood et al., 2011; Hauri et al., 2011; Barnes et al., 2013, 2014; Hui et al., 2013; Sharp et al., 2013; Tartese et al., 2013). Furthermore, recent studies have confirmed the presence of hydrous amphibole and apatite in many martian meteorites (i.e., Watson et al., 1994; Leshin, 2000; Boctor et al., 2003; Greenwood et al., 2008; McCubbin et al., 2009, 2010a, 2012; Hallis et al., 2012; Gross et al., 2013). In fact, recent estimates of H_2O abundances in the martian interior are similar to estimates of the terrestrial mantle (McCubbin et al., 2010a, 2012; Gross et al., 2013). Consequently, the question of whether there is a whitlockite component in planetary merrillite needs to be revisited in light of these findings. In the present study, we set out to find coexisting igneous apatite and merrillite in a martian meteorite to compare their volatile abundances and determine if a whitlockite component exists in martian merrillite.

Phosphate minerals have been reported in all martian meteorites (McSween and Treiman, 1998; Filiberto and Treiman, 2009b; Agee et al., 2013; Gross et al., 2013; McCubbin et al., 2013a), and they have also been identified on the martian surface by the Mars Exploration Rovers Spirit and Opportunity (see summaries of Gellert et al., 2006; Usui et al., 2008). We focus our efforts on the basaltic shergottite Shergotty because the apatite in it is known to have

elevated OH abundances, ranging from 4600-8600 ppm H_2O equivalent (all H concentrations in this manuscript are reported in the oxide component H_2O), the apatite coexists with merrillite, and the apatite and merrillite grains are large and appear to be igneous in origin (McCubbin et al., 2012).

Analytical methods

Electron probe microanalysis (EPMA)

EPMA was employed to conduct backscatter electron imaging on apatite and merrillite, and to quantitatively analyze merrillite in the Shergotty meteorite. Merrillite grains were analyzed using the JEOL JXA 8200 electron microprobe in the Institute of Meteoritics at the University of New Mexico (UNM), primarily following the phosphate EPMA procedure outlined by McCubbin et al. (2011; 2010c). An accelerating voltage of 15 kV and a nominal probe current of 25 nA was used during each analysis. In order to reduce or eliminate electron beam damage, we used a 20 μm spot for standardization and 2 to 20 μm diameter beams for analysis of merrillite grains in all the samples. We analyzed for P, Si, Ti, Ce, Y, Fe, Mn, Mg, Ca, Sr, and Na. All elements were standardized using Taylor standards as well as internal standards from the University of New Mexico. Specifically, F and Sr were standardized using Taylor strontium fluoride. Cl and Na were standardized using a scapolite crystal from the Smithsonian (Jarosewich et al., 1980). Ca and P were standardized using Durango apatite from (McCubbin et al. 2012), which also served as a secondary check on F and Cl. Ce and Y were standardized using their respective endmember orthophosphates (Donovan et al., 2003; Jarosewich and Boatner, 1991). Si and Mg were standardized using Taylor Olivine (from San Carlos, AZ). Mn was standardized using Taylor spessartine garnet. Ti was standardized on an ilmenite crystal from the Smithsonian

(USNM 133868). Na was standardized on Taylor albite, and Taylor chromite was used as a Fe standard.

To accurately measure the light element fluorine, a synthetic multilayer crystal with a large D-spacing (e.g., LDE-1) was used instead of the more classically used and widely available thallium acid phosphate (TAP) crystal because the intensity of the F Kα peak using the multilayer crystal is approximately 14 times more intense than with TAP (Potts and Tindle, 1989; Raudsepp, 1995; Reed, 2005). Stormer et al. (1993) documented that fluorine and chlorine X-ray count rates change with time during electron microprobe analysis of apatite as a function of crystallographic orientation. McCubbin et al. (2011; 2010c) revisited this problem with lunar samples and reported that fluorine count rates were not always constant during the course of an analysis; although, the changes in count rate did not appear to correlate with crystallographic orientation (determined on the basis of grain morphology). In the present study, we used the chart recorder function in the JEOL software to monitor for changes in F X-ray intensity in real time during each analysis (< 25 counts/second^2 (c/s^2), which is a similar approach outlined by Elardo et al. (2012) for apatite in lunar troctolite 76535.

The quality of merrillite analyses were assessed based on stoichiometric constraints and electron microprobe totals. If analytical totals were outside of the range 97.5-101.5 wt.%, the analysis was discarded. The leniency on analytical total deficiency is due to the possibility of up to 8500 ppm H_2O in whitlockite, which cannot be detected by the EPMA technique. In addition, the REE abundances of these martian merrillites are much less than lunar merrillites (Shearer et al., 2011; Jolliff et al., 2006), so we do not expect highly deficient totals from missing REE. If the stoichiometry of the tetrahedral site was over by more than 1% or deficient by more than 2% (i.e., +0.14 structural formula units (sfu) / -0.28 sfu on a 56 oxygen basis), the analysis was

discarded. The leniency on tetrahedral-site deficiency is due to the possibility of vacancy substitution for REE^{3+} in the merrillite Ca site (Hughes et al., 2006; Jolliff et al., 2006). The Ca, Na, and Mg sites can all have substantial vacancy and REE^{3+} substitution; therefore, analyses are only discarded on the basis of these cations if they overpopulate the total Ca, Na, Mg cation sites by 1% (i.e., 0.2 sfu on the basis of 56 oxygen atoms).

Secondary ion mass spectrometry (SIMS)

The measurements of F, OH, Cl, C, and S contents in Shergotty apatite and merrillite were performed on a Cameca 6f ion microprobe at the Department of Terrestrial Magnetism, at the Carnegie Institution of Washington in Washington, DC (Hauri et al., 2002) using a phosphate analysis routine from McCubbin et al. (2010b). Both the apatite and merrillite data were collected during the same session, but the apatite data were published separately in McCubbin et al. (2012). The focused (5-10 nA) 10kV Cs^+ primary ion beam was rastered on the sample to a 25 by 25 micron area. The secondary ion beam was extracted at -5 kV from an 8-micron diameter portion of the rastered area with a field aperture. An electron flood gun (-5 kV) was used to compensate for charge build up in the analysis area. A mass resolution of approximately 6000 was used to resolve $^{17.003}$[OH] from $^{16.999}$O. Standardization on five terrestrial apatites was performed at the beginning of the session. Information concerning the compositions of the standards used is presented in McCubbin et al. (2012), and the calibration curves for F, OH (reported as H_2O equivalent), Cl, and S are shown in Figure 1. The H_2O calibration curve resulted in 2σ relative uncertainties of about 3.3%. The 2σ relative uncertainties for Cl, F, and S were 2.3%, 1.7%, and 2.9%, respectively (Fig. 1). Each phosphate analysis lasted about 10 minutes. The detection limits for F, H_2O, Cl, and S were determined by analyzing a dry synthetic forsterite crystal (blank) that was mounted with our terrestrial apatite standards. The detection

158 limits for H_2O, Cl, and S were approximately 2 ppm, 0.1 ppm, and 0.5 ppm, respectively. The
159 number of F counts during the apatite analyses was too large to measure with the electron
160 multipliers, so F was analyzed using a faraday cup. The faraday cup has a significantly larger
161 background than the electron multipliers, which caused a high detection limit for F of
162 approximately 440 ppm. Because our standards were mounted in indium and we measured
163 minerals in an epoxy-mounted thin section, we also conducted analyses on pyroxene and
164 maskelynite in Shergotty to test whether our detection limits were reliable. These analyses are
165 also presented in Table 1 and generally agree with the detection limits determined by analysis of
166 dry synthetic forsterite.

167 Care was taken in the phosphate analyses to observe the direct ion image for $^{12.000}C$ for
168 every analysis location because grain boundaries and cracks within the sample are clearly
169 illuminated by carbon contamination on such surfaces. All of the phosphate grains contained
170 cracks; however, it was possible to obtain analyses on reasonably large areas of crack-free
171 phosphate within individual grains, and all of the data reported in Table 1 were obtained from
172 such crack-free areas.

173 Caution should be taken when SIMS analysis is carried out on epoxy mounted thin
174 sections because the possibility exists for OH contamination from the epoxy, which can invade
175 cracks in the sample that may not be visible in the ion probe optics. Therefore as a precaution,
176 epoxy from the Shergotty thin section was analyzed in the same way as our standards and
177 unknowns in order to determine C/OH ratios for the epoxy and estimate possible maximum H_2O
178 and Cl contributions from epoxy contamination on the surfaces of the thin section. Based on
179 these epoxy analyses and the measured C/OH ratios of our phosphates, if we assume that all of
180 the C in our phosphate analyses comes from epoxy, the maximum contribution is 2.5% of the

total H_2O for apatite and 0.5% of the total H_2O for merrillite. However, the lack of correlation between H_2O abundances and measured C/OH counts leads us to conclude that epoxy is not a major contributor to our measured C counts in the phosphates, which is an observation made previously on analyses of apatite from epoxy-mounted thin sections of lunar samples (McCubbin et al., 2010b). Therefore, the C in our analyses is most likely some combination of residual C from prior generations of C-coat, C contained in the phosphate mineral structure, and/or C-bearing mineral inclusions in the phosphate.

Results

Textural context of merrillite and apatite in Shergotty

We carried out petrographic observations of three thin sections of the Shergotty meteorite, and all of them are from the collection at the Institute of Meteoritics, UNM (Slides 408, 409 and 1142). Slide 1142 is a new slide that was made specifically for the present study. The phase assemblage of the Shergotty meteorite has been previously reported by Smith and Hervig (1979) and Stolper and McSween (1979). The description of the phase assemblage from those studies agrees with the observations of the present study and consists of pyroxene, maskelynite, magnetite, ilmenite, pyrrhotite, apatite, merrillite, fayalitic olivine, and silica. We focus here mainly on the textures relevant directly to the phosphates because detailed petrography about Shergotty already exists in previous studies. Apatites in Shergotty vary in crystal habit from euhedral to anhedral, with the euhedral grains being smaller (10-30μm) and occurring as mineral inclusions in pyroxene (Fig. 2a). The subhedral to anhedral apatite grains (Fig. 2b) are associated with late stage phases like silica, sulfides, and fayalitic olivine and seem to be constrained to the mesostasis (space interstitial to the earlier crystallized assemblage), which makes up approximately 3 to 5% of the mode (Stolper and McSween, 1979). Merrillite typically

occurs as subhedral to anhedral grains and is also commonly associated with late stage phases like silica, sulfides, and oxides (Fig. 2c, d). It is unclear whether merrillite or apatite crystallized first; however, only apatite is found as inclusions in pyroxenes, suggesting that at least some apatite crystallized early, possibly due to boundary layer effects around the growing pyroxene crystals (Harrison and Watson, 1984). There is more merrillite than apatite in the meteorite, with our estimate at a 1:2 apatite:merrillite modal ratio, which is similar to a previous estimate of 1:3 based on REE abundances in the bulk rock and the REE distributions between apatite and merrillite (Laul, 1987).

EPMA analysis of merrillite and apatite

Seventeen electron microprobe analyses of merrillite from Shergotty were collected in the present study, and the data were combined with seventy-three EPMA analyses of Shergotty apatite from McCubbin et al. (2012). Average apatite and merrillite compositions from Shergotty are reported in Table 2 along with calculated structural formulae. The 17 EPMA analyses of merrillite are available in an online supplementary Table (TableS1). A plot of the apatite X-site ternary components is presented in Figure 3, which shows good agreement between OH calculated by stoichiometry and that directly measured by SIMS. Furthermore, the apatites are Cl- and OH-rich similar to other apatites in basaltic shergottites (Filiberto and Treiman, 2009b; Greenwood et al., 2008; Leshin, 2000; McCubbin et al., 2012).

The major element chemistry of merrillite analyzed in this study is broadly consistent with previously published analyses of martian merrillite (Jolliff et al., 2006; Shearer et al., 2011). Structural formulae were calculated on the basis of 56 oxygens for merrillite and 13 total anions for apatite (see McCubbin et al., 2011 for discussion on cation versus anion normalization schemes). The merrillite structural formulae derived from our EPMA and SIMS analyses result

in good merrillite stoichiometry, with minimal whitlockite/bobdownsite components. Based on the SIMS data alone, there is a maximum of 4.5% whitlockite/bobdownsite components in Shergotty merrillite if the highest value is used for H_2O (196 ppm) and the detection limit is used for F (440 ppm).

SIMS Analysis of merrillite, pyroxene, and maskelynite

Three merrillite grains, one pyroxene grain, and one maskelynite were analyzed for OH, F, Cl, and S by secondary ion mass spectrometry (SIMS) in a single thin section of the Shergotty meteorite (UNM 1142). The H_2O content of the merrillite ranged from 53 to 196 ppm H_2O (Table 1). The fluorine abundances were all below detection, and Cl abundances ranged from below detection to 69 ppm Cl. Sulfur abundances ranged from 4 to 1285 ppm S, and seemed to correlate with irregular S hotspots that were observed in the ion image during some of the analyses, consistent with the presence of small S-rich mineral inclusions. Analytical uncertainties for H_2O, F, Cl, and S are reported in Table 1. The highest S abundances in Shergotty merrillite also correlated with elevated H_2O abundances (Table 1), so the H_2O analyses in merrillite with the least amount of S are most likely due to the H_2O in the merrillite structure.

Discussion

Does apatite in Shergotty coexist with merrillite or whitlockite?

Based on the SIMS data alone, there is a maximum of 4.5% non-merrillite (i.e., whitlockite or bobdownsite) component in Shergotty merrillite for a grain with the highest observed H_2O and F content at the detection limit. Based only on the EPMA results and the stoichiometric calculations, the elevated Na abundances and nearly full Ca(IIA)-site are more consistent with the crystal chemistry of merrillite versus whitlockite (Hughes et al., 2006; Jolliff et al., 2006). Therefore, both methods are in agreement that the Shergotty merrillite grains

measured during this study are consistent with the low H and F abundances characteristic of merrillite (i.e., no significant whitlockite or bobdownsite components). Importantly, the merrillite and apatite both appear to be igneous phases based on their textural occurrence and are not the result of post-magmatic alteration on the martian surface.

One post-magmatic process that has been postulated to affect volatile abundances of minerals is shock, and the Shergotty meteorite experienced high shock pressures (Stöffler et al., 1986; Aoudjehane et al., 2005). The effect of shock on devolatilization of minerals is largely unknown and experimental efforts to understand such effects have been difficult to interpret (Minitti et al., 2008a; Minitti et al., 2008b). However, we can use the stoichiometry of both phosphate phases to determine whether volatile-loss by shock is likely to have occurred for phosphates in Shergotty. In the case of apatite, the F, Cl, OH sums based on the SIMS indicate that the X-sites are fully occupied, which would not be the case if devolatilization due to shock had occurred. Stoichiometric volatile abundances of apatite and amphibole hosted by maskelynite in the Chassigny martian meteorite (Boctor et al., 2003; McCubbin and Nekvasil, 2008; McCubbin et al., 2010a) have also been used as evidence that devolatilization of volatile-rich minerals may not be common in martian meteorites. As discussed above, the presence of both substantial Na and Ca in the Shergotty merrillite Ca(IIA)-site are highly consistent with the crystal chemistry of merrillite versus whitlockite (Hughes et al., 2006; Jolliff et al., 2006) and strongly argues against the volatile abundances of merrillite having been affected by the high shock pressure experienced by Shergotty as loss of H, F, and Cl would have left structural vacancies in equal proportion to the amount of lost atoms in both mineral phases. Consequently, the hydrated nature of apatite and dry nature of merrillite in Shergotty is likely a primary magmatic feature.

Does the presence of merrillite imply low H abundances in magmas?

The presence of merrillite has often been used as evidence for low H abundances in magmatic systems (i.e., Smith and Hervig, 1979; Sha, 2000; Ionov et al., 2006; Patiño-Douce and Roden, 2006; Hughes et al., 2008; Patiño-Douce et al., 2011;), but this assertion clearly needs to be reassessed in light of the results from the present study where merrillite coexists with OH-rich apatite. Based on recent apatite-melt partitioning experiments on shergottitic liquids, the halogens play a much larger role in stabilizing magmatic apatite than H. In fact, apatite prefers F over OH by a factor of approximately 100, and it prefers Cl over OH by a factor of about 20 (McCubbin et al., 2013c, 2014; Vander Kaaden et al., 2012). Furthermore, estimates for apatite/melt partition coefficients for H_2O typically range from 0.03-0.3 (Mathez and Webster, 2005; McCubbin et al., 2010b, 2014; Vander Kaaden et al., 2012), indicating that H_2O is somewhat incompatible in apatite. Consequently, relatively high abundances of H_2O may be required in the melt to stabilize OH-rich apatite over merrillite. The presence of merrillite in magmatic systems likely has more to do with the ratio of phosphorus to halogens in silicate liquids, with H playing a subordinate role to the halogens in the apatite-melt system, an idea first proposed by Patiño-Douce and Roden, (2006) and supported by recent work on apatite-melt partitioning relationships. If the ratio of P to F+Cl controls the stability of apatite relative to merrillite, the presence of merrillite would either indicate that the system is depleted in halogens or enriched in phosphorus (Patiño-Douce and Roden, 2006). Mars is inferred to have high P abundances in its bulk silicate (crust and mantle) compared to other planetary bodies (Dreibus and Wanke, 1985; Wanke and Dreibus, 1994) and also appears to be somewhat depleted in fluorine (McCubbin et al., 2013b), which could explain why merrillite is a ubiquitous phosphate phase in martian basalts despite substantial evidence supporting elevated H and Cl abundances in

martian magmas (Filiberto and Treiman, 2009a; b; Gross et al., 2013; McCubbin et al., 2013a; McCubbin et al., 2012; McCubbin et al., 2009; McSween et al., 2001). Additional experimental work is required to determine the controls of apatite versus merrillite stability in silicate melts, but based on the work presented here, H_2O is not likely a primary limiting factor.

Whitlockite components in magmatic merrillite

It has been postulated that whitlockite and whitlockite components in merrillite are unique to Earth and may not be found in other planetary materials (Hughes et al., 2008). The results of the present study seem to support this claim, although a reason for the observation has not yet been described. Based on the OH abundances in apatite, the residual Shergotty melt would have had 1.5-3.0 wt.% H_2O at the time of phosphate crystallization (McCubbin et al., 2012). If merrillite and whitlockite form a solid solution (as demonstrated by Hughes et al., 2008), it seems reasonable that the merrillite forming from this H-rich liquid should have a larger whitlockite component than 0.5-2.5%. However, the geologic environments in which whitlockite and bobdownsite are commonly found on Earth tend to be low temperature systems (<500 °C) such as pegmatites and hydrothermal environments (Calvo and Gopal, 1975; Frondel, 1941; Jolliff et al., 2006; Tait et al., 2011), where the stability of whitlockite has already been proven experimentally (Hughes et al., 2008). In fact, Hughes et al. (2008) demonstrated that at 1050 °C, whitlockite completely dehydrogenates to merrillite, but whitlockite is stable at 500 °C. Consequently, the high-temperature igneous systems in many extraterrestrial planetary bodies will preclude the magmatic mixing of merrillite and whitlockite components if the solidus is above the upper thermal stability limit of whitlockite components in merrillite (<1050°C). Additional experiments on whitlockite thermal stability are needed to better establish where in the range of 500-1050 °C whitlockite is no longer stable. In fact, the presence of a whitlockite

component in planetary merrillite may be an important indicator of secondary alteration processes by aqueous or hydrothermal fluids on other planetary bodies. At this point in time, the observation of a measurable whitlockite component in merrillite is still unique to the Earth, but given what we understand about whitlockite stability, the occurrence of a whitlockite component in extraterrestrial material should not be unexpected, particularly in low-T hydrothermal-type environments.

Implications

Merrillite remains one of the minerals with great potential for deciphering magmatic crystallization conditions in planetary science, and there are still far more questions about merrillite than answers. For example, it is not clear why merrillite is ubiquitous in extraterrestrial samples and rare in terrestrial rocks. Is this difference telling us something fundamental about the geochemistry of Earth compared to the rest of the inner Solar System? What factors control the stability of merrillite over apatite? The present study predicts that the halogen/phosphorus ratio plays the largest role in determining saturation in apatite versus whitlockite, which was also predicted by thermodynamic calculations by Patiño-Douce and Roden, (2006); however, experimental work is required to determine the compositional boundaries in the apatite-merrillite-melt system. Although many questions about merrillite remain, the present study argues strongly against the interpretation that merrillite can be used as an indicator of a dry magmatic system. Despite its apathy to magmatic H contents at elevated temperatures, merrillite still holds promise as an important accessory mineral given its affinity for REE, and it could become a powerful tool for understanding late stage magmatic processes once its crystal chemical behavior is better characterized.

Acknowledgements

We thank the meteorite museum in the Institute of Meteoritics at the University of New Mexico for allocating thin sections of the Shergotty meteorite. We would like to thank Dr. Bradley Jolliff and Dr. Juliane Gross for very helpful and thorough reviews of the manuscript, and we would also like to acknowledge Dr. Steven Simon for his efforts as the Associate Editor. This work was funded by the NASA Mars Fundamental Research Program grant NNX13AG44G to FMM and NASA Cosmochemistry grant NNX13AH85G to CKS. SME acknowledges support from NASA Earth and Space Science Fellowship NNX12AO15H awarded to SME and a graduate fellowship from the NM Space Grant Consortium.

References cited

Agee, C.B., Wilson, N.V., McCubbin, F.M., Ziegler, K., Polyak, V.J., Sharp, Z.D., Asmerom, Y., Nunn, M.H., Shaheen, R., Thiemens, M.H., Steele, A., Fogel, M.L., Bowden, R., Glamoclija, M., Zhang, Z., and Elardo, S.M. (2013) Unique meteorite from early Amazonian Mars: Water-rich basaltic breccia Northwest Africa 7034. Science, 339, 780-785.

Aoudjehane, H.C., Jambon, A., Reynard, B., and Blanc, P. (2005) Silica as a shock index in shergottites: A cathodoluminescence study. Meteoritics & Planetary Science, 40, 967-979.

Barnes, J.J., Franchi, I.A., Anand, M., Tartese, R., Starkey, N.A., Koike, M., Sano, Y., and Russell, S.S. (2013) Accurate and precise measurements of the D/H ratio and hydroxyl content in lunar apatites using NanoSIMS. Chemical Geology, 337-338, 48-55.

Barnes, J.J., Tartese, R., Anand, M., McCubbin, F.M., Franchi, I.A., Starkey, N.A., and Russell, S.S. (2014) The origin of water in the primitive Moon as revealed by the lunar highlands samples. Earth and Planetary Science Letters, 390, 244-252.

Boctor, N.Z., Alexander, C.M.O., Wang, J., and Hauri, E. (2003) The sources of water in martian meteorites: Clues from hydrogen isotopes. Geochimica et Cosmochimica Acta, 67, 3971-3989.

Boyce, J.W., Liu, Y., Rossman, G.R., Guan, Y., Eiler, J.M., Stolper, E.M., and Taylor, L.A. (2010) Lunar apatite with terrestrial volatile abundances. Nature, 466, 466-469.

Calvo, C., and Gopal, R. (1975) Crystal structure of whitlockite from Palmero Quarry. American Mineralogist, 60, 120-133.

Donovan, J.J., Hanchar, J.M., Picolli, P.M., Schrier, M.D., Boatner, L.A., and Jarosewich, E. (2003) A re-examination of the rare-earth-element orthophosphate standards in use for electron-microprobe analysis. Canadian Mineralogist, 41, 221-232.

Dreibus, G., and Wanke, H. (1985) Mars, a volatile-rich planet. Meteoritics, 20, 367-381.

Elardo, S.M., McCubbin, F.M., and Shearer, C.K. (2012) Chromite symplectites in Mg-suite troctolite 76535 as evidence for infiltration metasomatism of a lunar layered intrusion. Geochimica et Cosmochimica Acta, 87, 154-177.

379 Filiberto, J., and Treiman, A.H. (2009a) The effect of chlorine on the liquidus of basalt: First
380 results and implications for basalt genesis on Mars and Earth. Chemical Geology, 263,
381 60-68.
382 Filiberto, J., and Treiman, A.H. (2009b) Martian magmas contained abundant chlorine, but little
383 water. Geology, 37, 1087-1090.
384 Frondel, C. (1941) Whitlockite a new calcium phosphate, $Ca_3(PO4)_2$. American Mineralogist,
385 26, 145-152.
386 Gellert, R., Rieder, R., Bruckner, J., Clark, B.C., Dreibus, G., Klingelhofer, G., Lugmair, G.,
387 Ming, D.W., Wanke, H., Yen, A., Zipfel, J., and Squyres, S.W. (2006) Alpha particle X-
388 ray spectrometer (APXS): Results from Gusev crater and calibration report. Journal of
389 Geophysical Research-Planets, 111, DOI: 10.1029/2005JE002555.
390 Greenwood, J.P., Itoh, S., Sakamoto, N., Vicenzi, E.P., and Yurimoto, H. (2008) Hydrogen
391 isotope evidence for loss of water from Mars through time. Geophysical Research
392 Letters, 35, DOI: 10.1029/2007GL032721.
393 Greenwood, J.P., Itoh, S., Sakamoto, N., Warren, P., Taylor, L., and Yurimoto, H. (2011)
394 Hydrogen isotope ratios in lunar rocks indicate delivery of cometary water to the Moon.
395 Nature Geoscience, 4, 79-82.
396 Gross, J., Filiberto, J., and Bell, A.S. (2013) Water in the martian interior: Evidence for
397 terrestrial MORB mantle-like volatile contents from hydroxyl-rich apatite in olivine–
398 phyric shergottite NWA 6234. Earth and Planetary Science Letters, 369–370, 120-128.
399 Hallis, L.J., Taylor, G.J., Nagashima, K., and Huss, G.R. (2012) Magmatic water in the martian
400 meteorite Nakhla. Earth and Planetary Science Letters, 359–360, 84-92.
401 Harrison, T.M., and Watson, E.B. (1984) The behavior of apatite during crustal anatexis:
402 Equilibrium and kinetic considerations. Geochimica et Cosmochimica Acta, 48, 1467-
403 1477.
404 Hauri, E., Wang, J.H., Dixon, J.E., King, P.L., Mandeville, C., and Newman, S. (2002) SIMS
405 analysis of volatiles in silicate glasses 1. Calibration, matrix effects and comparisons with
406 FTIR. Chemical Geology, 183, 99-114.
407 Hauri, E.H., Weinreich, T., Saal, A.E., Rutherford, M.J., and Van Orman, J.A. (2011) High pre-
408 eruptive water contents preserved in lunar melt inclusions. Science, 333, 213-215.
409 Hughes, J.M., Jolliff, B.L., and Gunter, M.E. (2006) The atomic arrangement of merrillite from
410 the Fra Mauro Formation, Apollo 14 lunar mission: The first structure of merrillite from
411 the Moon. American Mineralogist, 91, 1547-1552.
412 Hughes, J.M., Jolliff, B.L., and Rakovan, J. (2008) The crystal chemistry of whitlockite and
413 merrillite and the dehydrogenation of whitlockite to merrillite. American Mineralogist,
414 93, 1300-1305.
415 Hui, H., Peslier, A.H., Zhang, Y., and Neal, C.R. (2013) Water in lunar anorthosites and
416 evidence for a wet early Moon. Nature Geosciences, 6, 177-180.
417 Ionov, D.A., Hofmann, A.W., Merlet, C., Gurenko, A.A., Hellebrand, E., Montagnac, G., Gillet,
418 P., and Prikhodko, V.S. (2006) Discovery of whitlockite in mantle xenoliths: Inferences
419 for water- and halogen-poor fluids and trace element residence in the terrestrial upper
420 mantle. Earth and Planetary Science Letters, 244, 201-217.
421 Jarosewich, E., and Boatner, L.A. (1991) Rare Earth element reference samples for electron
422 microprobe analysis. Geostandards Newsletter, 15, 397-399.
423 Jarosewich, E., Nelen, J.A., and Norberg, J.A. (1980) Reference Samples for Electron
424 Microprobe Analysis. Geostandards Newsletter, 4, 43-47.

Jolliff, B.L., Haskin, L.A., Colson, R.O., and Wadhwa, M. (1993) Partitioning in REE-saturating minerals - theory, experiment, and modeling of whitlockite, apatite, and evolution of lunar residual magmas. Geochimica et Cosmochimica Acta, 57, 4069-4094.

Jolliff, B.L., Hughes, J.M., Freeman, J.J., and Zeigler, R.A. (2006) Crystal chemistry of lunar merrillite and comparison to other meteoritic and planetary suites of whitlockite and merrillite. American Mineralogist, 91, 1583-1595.

Laul, J.C. (1987) Rare earth patterns in shergottite phosphates and residues. Journal of Geophysical Research-Solid Earth and Planets, 92, E633-E640.

Leshin, L.A. (2000) Insights into martian water reservoirs from analyses of martian meteorite QUE94201. Geophysical Research Letters, 27, 2017-2020.

Mathez, E.A., and Webster, J.D. (2005) Partitioning behavior of chlorine and fluorine in the system apatite-silicate melt-fluid. Geochimica et Cosmochimica Acta, 69, 1275-1286.

McCubbin, F.M., and Nekvasil, H. (2008) Maskelynite-hosted apatite in the Chassigny meteorite: Insights into late-stage magmatic volatile evolution in martian magmas. American Mineralogist, 93, 676-684.

McCubbin, F.M., Tosca, N.J., Smirnov, A., Nekvasil, H., Steele, A., Fries, M., and Lindsley, D.H. (2009) Hydrothermal jarosite and hematite in a pyroxene-hosted melt inclusion in martian meteorite Miller Range (MIL) 03346: Implications for magmatic-hydrothermal fluids on Mars. Geochimica et Cosmochimica Acta, 73, 4907-4917.

McCubbin, F.M., Smirnov, A., Nekvasil, H., Wang, J., Hauri, E., and Lindsley, D.H. (2010a) Hydrous magmatism on Mars: A source of water for the surface and subsurface during the Amazonian. Earth and Planetary Science Letters, 292, 132-138.

McCubbin, F.M., Steele, A., Hauri, E.H., Nekvasil, H., Yamashita, S., and Hemley, R.J. (2010b) Nominally hydrous magmatism on the Moon. Proceedings of the National Academy of Science, 107, 11223-11228.

McCubbin, F.M., Steele, A., Nekvasil, H., Schnieders, A., Rose, T., Fries, M., Carpenter, P.K., and Jolliff, B.L. (2010c) Detection of structurally bound hydroxyl in fluorapatite from Apollo mare basalt 15058,128 using TOF-SIMS. American Mineralogist, 95, 1141-1150.

McCubbin, F.M., Jolliff, B.L., Nekvasil, H., Carpenter, P.K., Zeigler, R.A., Steele, A., Elardo, S.M., and Lindsley, D.H. (2011) Fluorine and chlorine abundances in lunar apatite: Implications for heterogeneous distributions of magmatic volatiles in the lunar interior. Geochimica et Cosmochimica Acta, 75, 5073-5093.

McCubbin, F.M., Hauri, E.H., Elardo, S.M., Vander Kaaden, K.E., Wang, J., and Shearer, C.K. (2012) Hydrous melting of the martian mantle produced both depleted and enriched shergottites. Geology, 40, 683-686.

McCubbin, F.M., Elardo, S.M., Shearer Jr, C.K., Smirnov, A., Hauri, E.H., and Draper, D.S. (2013a) A petrogenetic model for the co-magmatic origin of chassignites and nakhlites: Inferences from chlorine-rich minerals, petrology, and geochemistry. Meteoritics and Planetary Sciences, 48, 819-853.

McCubbin, F.M., Jones, R.H., Shearer Jr, C.K., Elardo, S.M., Agee, C.B., Santos, A.R., Burger, P.V., Bell, A.S., and Papike, J.J. (2013b) The volatile chemistry of apatite in planetary materials: Implications for the behavior of volatiles during planetary differentiation? Proceedings of the 44th Lunar and Planetary Science Conference, p. #2731. Lunar and Planetary Institute, Woodlands, TX.

McCubbin, F.M., Vander Kaaden, K.E., Whitson, E.S., Bell, A.S., and Shearer Jr, C.K. (2013c) Partitioning of F and Cl between apatite and a synthetic shergottite liquid (QUE 94201) at

1 and 4 GPa from 950 to 1450 C. 44th Lunar and Planetary Science Conference, p. # 2748. Lunar and Planetary Institute, Woodlands, TX.

McSween, H.Y., Grove, T.L., Lentz, R.C.F., Dann, J.C., Holzheid, A.H., Riciputi, L.R., and Ryan, J.G. (2001) Geochemical evidence for magmatic water within Mars from pyroxenes in the Shergotty meteorite. Nature, 409, 487-490.

McSween, H.Y., and Treiman, A.H. (1998) Martian meteorites. In J. J. Papike, Eds., Planetary Materials, 36, p. F1-F53. Reviews in Mineralogy and Geochemistry, Mineralogical Society of America, Washington, D.C.

Minitti, M.E., Leshin, L.A., Dyar, M.D., Ahrens, T.J., Guan, Y., and Luo, S.N. (2008a) Assessment of shock effects on amphibole water contents and hydrogen isotope compositions: 2. Kaersutitic amphibole experiments. Earth and Planetary Science Letters, 266, 288-302.

Minitti, M.E., Rutherford, M.J., Taylor, B.E., Dyar, M.D., and Schultz, P.H. (2008b) Assessment of shock effects on amphibole water contents and hydrogen isotope compositions: 1. Amphibolite experiments. Earth and Planetary Science Letters, 266, 46-60.

Patiño Douce, A.E., and Roden, M.F. (2006) Apatite as a probe of halogen and water fugacities in the terrestrial planets. Geochimica et Cosmochimica Acta, 70, 3173-3196.

Patiño Douce, A.E., Roden, M.F., Chaumba, J., Fleisher, C., and Yogodzinski, G. (2011) Compositional variability of terrestrial mantle apatites, thermodynamic modeling of apatite volatile contents, and the halogen and water budgets of planetary mantles. Chemical Geology, 288, 14-31.

Piccoli, P.M., and Candela, P.A. (2002) Apatite in igneous systems. In M. J. Kohn, J. Rakovan, and J. M. Hughes Eds., Phosphates: Geochemical, Geobiological, and Materials Importance, 48, p. 255-292. Reviews in Mineralogy and Geochemistry, Mineralogical Society of America, Washington, D.C.

Potts, P.J., and Tindle, A.G. (1989) Analytical characteristics of a multilayer dispersion element (2D =60Å) in the determination of fluorine in minerals by electron microprobe. Mineralogical Magazine, 53(371), 357-362.

Raudsepp, M. (1995) Recent advances in the electron microprobe microanalysis of minerals for the light elements. Canadian Mineralogist, 33, 203-218.

Reed, S.J.B. (2005) Electron Microprobe Analysis and Scanning Electron Microscopy in Geology. 192 p. Cambridge University Press, Cambridge.

Rubin, A.E. (1997) Mineralogy of meteorite groups. Meteoritics & Planetary Science, 32, 231-247.

Saal, A.E., Hauri, E.H., Cascio, M.L., Van Orman, J.A., Rutherford, M.C., and Cooper, R.F. (2008) Volatile content of lunar volcanic glasses and the presence of water in the Moon's interior Nature, 454, 192-195.

Saal, A.E., Hauri, E.H., Van Orman, J.A., and Rutherford, M.A. (2013) Hydrogen isotopes in lunar volcanic glasses and melt inclusions reveal a carbonaceous chondrite heritage. Science, 340, 1317-1320.

Sha, L.K. (2000) Whitlockite solubility in silicate melts: Some insights into lunar and planetary evolution. Geochimica et Cosmochimica Acta, 64, 3217-3236.

Sharp, Z.D., McCubbin, F.M., and Shearer, C.K. (2013) A hydrogen-based oxidation mechanism relevant to planetary formation. Earth and Planetary Science Letters, 380, 88-97.

Shearer, C.K., Papike, J.J., Burger, P.V., Sutton, S.R., McCubbin, F.M., and Newville, M. (2011) Direct determination of europium valence state by XANES in extraterrestrial merrillite.

Implications for REE crystal chemistry and martian magmatism. American Mineralogist, 96, 1418-1421.

Smith, J.V., and Hervig, R.L. (1979) Shergotty meteorite: Mineralogy, petrography, and minor elements. Meteoritics, 14, 121-142.

Stoffler, D., Ostertag, R., Jammes, C., Pfannschmidt, G., Gupta, P.R.S., Simon, S.B., Papike, J.J., and Beauchamp, R.H. (1986) Shock metamorphism and petrography of the Shergotty achondrite. Geochimica et Cosmochimica Acta, 50, 889-903.

Stolper, E., and McSween, H.Y. (1979) Petrology and origin of the Shergottite meteorites. Geochimica et Cosmochimica Acta, 43, 1475-1498.

Stormer, J.C., Pierson, M.L., and Tacker, R.C. (1993) Variation of F-X-ray and Cl-X-ray intensity due to anisotropic diffusion in apatite during electron-microprobe analysis. American Mineralogist, 78(5-6), 641-648.

Tait, K.T., Barkley, M.C., Thompson, R.M., Origlieri, M.J., Evans, S.H., Prewitt, C.T., and Yang, H. (2011) Bobdownsite, a new mineral species from Big Fish River, Yukon, Canada and its structural relationship with whitlockite-type compounds. Canadian Mineralogist, 49, 1065-1078.

Tartese, R., Anand, M., Barnes, J.J., Starkey, N.A., Franchi, I.A., and Sano, Y. (2013) The abundance, distribution, and isotopic composition of hydrogen in the Moon as revealed by basaltic lunar samples: implications for the volatile inventory of the Moon. Geochimica et Cosmochimica Acta, 122, 58-74.

Usui, T., McSween, H.Y., and Clark, B.C. (2008) Petrogenesis of high-phosphorous Wishstone Class rocks in Gusev Crater, Mars. Journal of Geophysical Research-Planets, 113(E12), 13.

Vander Kaaden, K.E., McCubbin, F.M., Whitson, E.S., Hauri, E.H., and Wang, J. (2012) Partitioning of F, Cl, and H_2O between apatite and a synthetic Shergottite liquid (QUE 94201) at 1.0 GPa and 990-1000^{o}C. 43rd Lunar and Planetary Science Conference, p. #1247. Lunar and Planetary Institute, Houston, TX.

Wanke, H., and Dreibus, G. (1994) Chemistry and accretion history of Mars. Philosophical Transactions of the Royal Society of London Series a-Mathematical Physical and Engineering Sciences, 349, 285-293.

Watson, L.L., Hutcheon, I.D., Epstein, S., and Stolper, E.M. (1994) Water on Mars: Clues from deuterium/hydrogen and water contents of hydrous phases in SNC meteorites. Science, 265, 86-90.

Figure captions

Figure 1. Calibration curves determined for quantifying water, fluorine, chlorine, and sulfur contents of phosphates by SIMS (adopted from McCubbin et al., 2012). The data points used to construct the curve were from five terrestrial apatite standards and a volatile-free synthetic forsterite. The regression line is forced to the origin because the detection limit of our analysis routine is approximately 3 ppm or less (with the exception of fluorine which was analyzed with the faraday cup, resulting in a detection limit for fluorine of approximately 440 ppm as determined by analysis of the dry synthetic forsterite. The 2σ error for the slope of each calibration curve is presented parenthetically.

Figure 2. High-resolution back-scattered electron images of apatite and merrillite from Shergotty a) Apatite b) Apatite c) Merrillite d) Merrillite. All phases present are identified, and the phase abbreviations are indicated as follows: Ap = Apatite, Me = Merrillite, Ti-Mt = Titanomagnetite, Ilm = ilmenite, Fa = fayalitic olivine, Msk = maskelynite, Cpx = Clinopyroxene, Si = Silica, and Po = pyrrhotite.

Figure 3. Ternary plot of apatite X-site occupancy (mol%) from the Shergotty meteorite using EPMA (black points) and SIMS (gray points) data collected by McCubbin et al. (2012). OH component calculated by stoichiometry from EPMA data assuming 1 – Cl – F = OH (structural formula units).

589
590

Table 1: Secondary ion mass spectrometry analyses of mineral phases from Shergotty

Analysis[a]	F (ppm)[b]	Cl (ppm)[b]	H_2O (ppm)[b]	S (ppm)[b]
Merrillite1_1	<440	<0.1	54 ± 2	4 ± 0.12
Merrillite2_1	<440	69 ± 1.6	196 ± 7	1285 ± 38
Merrillite3_1	<440	3 ± 0.07	53 ± 2	55 ± 1.6
Merrillite3_2	<440	28 ± 0.64	134 ± 4	705 ± 21
Merrillite3_3	<440	14 ± 0.32	65 ± 2	661 ± 19
Pyroxene1_1	<440	0.72 ± 0.02	6.2 ± 0.2	7.5 ± 0.22
Pyroxene1_2	<440	0.72 ± 0.02	6.2 ± 0.2	7.5 ± 0.22
Maskelynite1_1	<440	0.13 ± 0.00	14.1 ± 0.5	1.5 ± 0.04
Maskelynite1_2	<440	<0.1	2.4 ± 0.1	<0.1
Analysis[a]	F (wt.%)[b]	Cl (wt.%)[b]	H_2O (wt.%)[b]	S (ppm)[b]
Apatite_1	1.46 ± 0.02	1.92 ± 0.04	0.65 ± 0.02	732 ± 22
Apatite_2	1.48 ± 0.03	1.74 ± 0.04	0.53 ± 0.02	614 ± 18
Apatite _3	1.38 ± 0.02	2.11 ± 0.05	0.55 ± 0.02	790 ± 23
Apatite _4	1.39 ± 0.02	1.77 ± 0.04	0.59 ± 0.02	588 ± 17
Apatite _5	1.18 ± 0.02	1.96 ± 0.04	0.78 ± 0.03	637 ± 19
Apatite _6	1.37 ± 0.02	2.33 ± 0.05	0.71 ± 0.02	626 ± 18
Apatite _7	1.53 ± 0.03	2.12 ± 0.05	0.52 ± 0.02	659 ± 19
Apatite _8	1.48 ± 0.03	2.09 ± 0.05	0.46 ± 0.02	583 ± 17
Apatite _9	0.42 ± 0.01	3.12 ± 0.07	0.86 ± 0.03	446 ± 13

Apatite analyses published in McCubbin et al. (2012)
"-" used to indicate that something was not measured
b.d. – indicates below detection limit
[a]Analysis number and analyzed mineral are indicated for each analysis.
[b]All reported uncertainties are 2σ
[c]Fluorine was analyzed using an electron multiplier, resulting in an elevated detection limit of about 440 ppm F. Detection limits for H_2O were near 2 ppm, and Cl and S detection limits were approximately 0.1 ppm and 0.45 ppm respectively.

591
592
593
594
595
596
597
598
599
600
601
602
603

604
605

Table 2: Average electron microprobe analyses of apatite and merrillite from Shergotty

Oxide	**Apatite (N=73)**	**Merrillite (N=17)**
P_2O_5	41.17 (53)	44.99 (57)
SiO_2	0.65 (33)	<0.10
TiO2	-	<0.05
Ce_2O_3	0.03 (2)	0.09 (1)
Y_2O_3	0.02 (1)	0.12 (3)
FeO	1.21 (50)	4.12 (18)
MnO	-	0.13 (2)
MgO	0.03 (2)	1.83 (2)
CaO	54.21 (70)	47.33 (8)
SrO	-	<0.06
Na_2O	0.09 (5)	1.24 (8)
SO_3	0.21 (18)	-
F[b]	0.98 (58)	-
Cl[b]	2.5 (1.3)	-
-O ≡ F	0.41	-
-O ≡ Cl	0.56	-
Total	**100.13**	**99.85**
Structural formulae based on 13 total anions for apatite and 56 total oxygens for merrillite		
P	2.95	13.89
Si	0.05	
Ti	-	
Ce	0.00	0.01
Y	0.00	0.02
Fe	0.09	1.26
Mn	-	0.04
Mg	0.00	0.99
Ca	4.92	18.52
Sr	-	
Na	0.01	0.88
S	0.01	-
∑Cations	**8.03**	**35.61**
F	0.26	-
Cl	0.36	-
∑Anions	**0.62**	**-**
H[a]	0.38	-

1σ Standard deviation of the mean presented parenthetically next to each value.
Apatite analyses are from McCubbin et al., (2012)
"-" used to indicate that something was not measured
[a] Calculated assuming that F + Cl + H = 1 apfu
[b]Large standard deviation was related to grain-grain variability in the sample (see Figure 3).
Detection limits for all elements reported in Table S1.

606
607
608
609
610

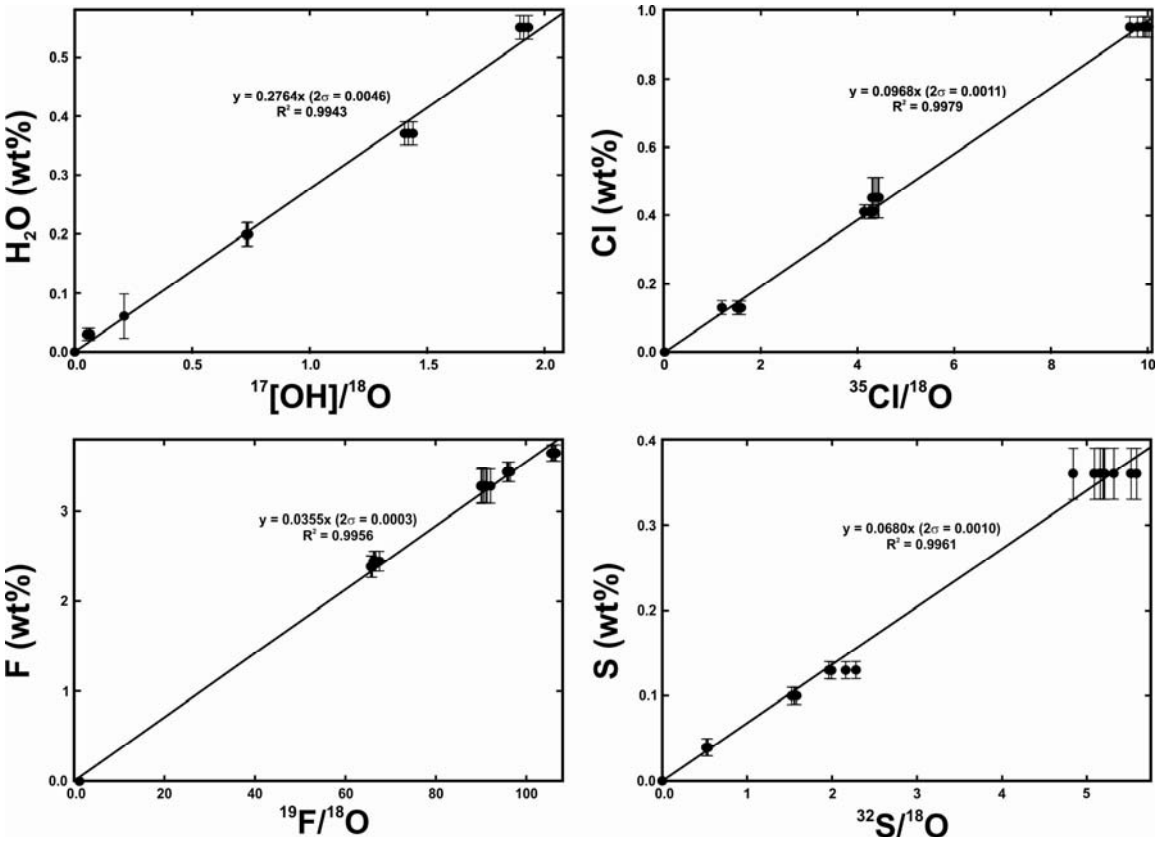

Figure 1. Calibration curves determined for quantifying water, fluorine, chlorine, and sulfur contents of phosphates by SIMS (adopted from McCubbin et al., 2012). The data points used to construct the curve were from five terrestrial apatite standards and a volatile-free synthetic forsterite. The regression line is forced to the origin because the detection limit of our analysis routine is approximately 3 ppm or less (with the exception of fluorine which was analyzed with the faraday cup, resulting in a detection limit for fluorine of approximately 450 ppm as determined by analysis of the dry synthetic forsterite). The 2σ error for the slope of each calibration curve is presented parenthetically.

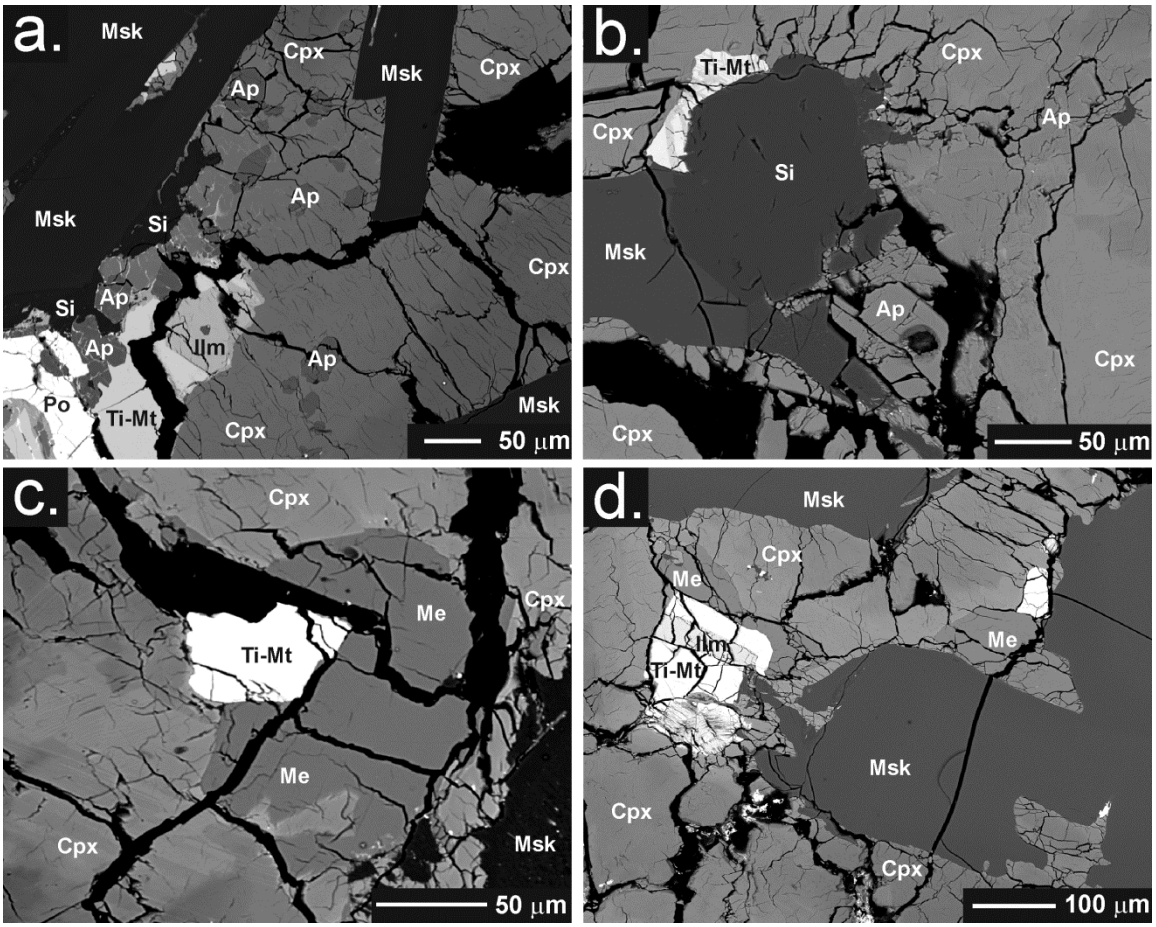

Figure 2. High-resolution back-scattered electron images of apatite and merrillite from Shergotty a) Apatite b) Apatite c) Merrillite d) Merrillite All phases present are identified, and the phase abbreviations are indicated as follows: Ap = Apatite, Me = Merrillite, Ti-Mt = Titanomagnetite, Ilm = ilmenite, Fa = fayalitic olivine, Msk = maskelynite, Cpx = Clinopyroxene, Si = Silica, and Po = pyrrhotite.

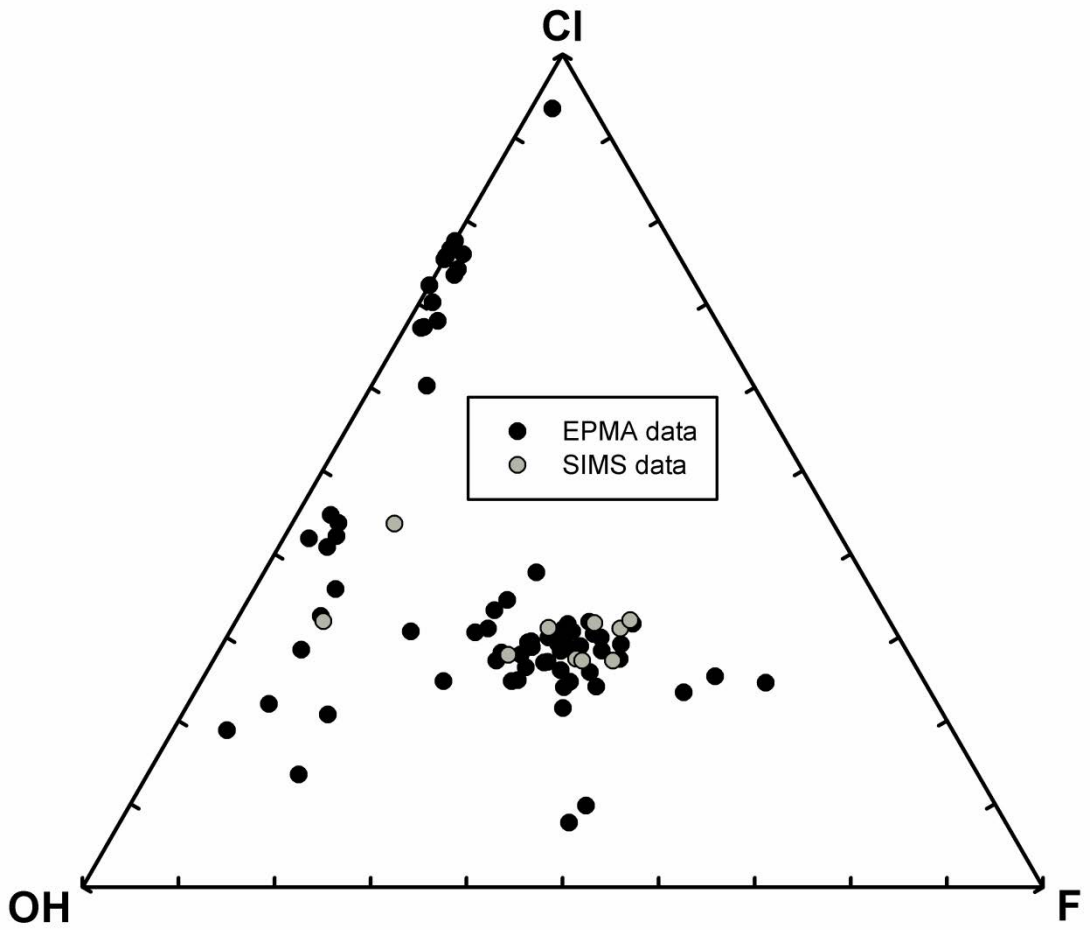

Figure 3. Ternary plot of apatite X-site occupancy (mol%) from the Shergotty meteorite using EPMA (black points) and SIMS (gray points) data collected by McCubbin et al. (2012). OH component calculated by stoichiometry from EPMA data assuming 1 – Cl – F = OH (structural formula units).